Planta (2000) 210: 205–214

Planta

A nonphotochemical-quenching-deficient mutant of *Arabidopsis thaliana* possessing normal pigment composition and xanthophyll-cycle activity

Richard B. Peterson, Evelyn A. Havir

Department of Biochemistry and Genetics, The Connecticut Agricultural Experiment Station, 123 Huntington St., New Haven, CT 06511, USA

Received: 26 May 1999 / Accepted: 17 June 1999

Abstract. Higher-plant chloroplasts alter the distribution of absorbed radiant energy between photosynthesis and heat formation in response to changing illumination level or environmental stress. Fluorescence imaging was used to screen 62 yellow-green T-DNA insertion mutant lines of *Arabidopsis thaliana* (L.) Heynh. for reduced photoprotective nonphotochemical quenching (NPQ) capacity. Pulse-modulation fluorometry was employed to characterize one line (denoted Lsr1$^-$) that exhibited an approximately 50% reduction in NPQ compared to the wild type (WT). The loss in NPQ capacity was associated with the ΔpH-dependent phase of quenching (qE). Under the growth conditions employed, pigment composition and levels of the six photosystem-II light-harvesting chlorophyll *a*/*b* proteins were identical in mutant and WT. Changes in the in-vivo levels of the xanthophyll pigments violaxanthin, antheraxanthin, and zeaxanthin in excess light were the same for mutant and WT. However, use of the violaxanthin de-epoxidase inhibitor dithiothreitol indicated that a zeaxanthin-dependent component of NPQ was specifically reduced in the mutant. The mutant exhibited diminished suppression of minimum fluorescence yield (F_o) in intense light suggesting an altered threshold in the mechanism of response to light stress in the mutant. The NPQ-deficient phenotype was meiotically transmissible as a semi-dominant trait and mapped near marker T27K12 on chromosome 1. The results suggest that the mutant is defective in sensing the transthylakoid ΔpH that reports exposure to excessive illumination.

Key words: *Arabidopsis* (photosynthesis) – Energy dissipation – Mutant (*Arabidopsis*) – Photosynthesis – Photosystem II – Zeaxanthin

Introduction

Higher plants and algae rely on photosynthesis as the sole means of energy input for growth. Consequently, chloroplasts typically possess efficient light-harvesting systems to maximize light capture and similarly effective photochemical mechanisms which enable autotrophic growth even in low light. These adaptations can lead to overstimulation and photoinactivation of PSII reaction centers at high light levels or when CO_2-fixing capacity is restricted due to environmental stress (Horton et al. 1996). The mechanism of photoinactivation appears to be associated with the oxidation-reduction state of the PSII acceptor Q_A (Melis 1999). When Q_A is reduced, excitation of PSII can result in formation of reactive singlet O_2. Attack of the D1 protein of the PSII reaction center by active oxygen results in permanent damage so that removal and replacement of the D1 polypeptide is necessary to restore function to the center.

Chloroplasts possess a reversible photoprotective mechanism to safely dissipate excessive absorbed light as harmless heat. This process, termed nonphotochemical quenching (NPQ), requires a transthylakoid membrane pH gradient (ΔpH) and is strongly associated with accumulation of de-epoxidized xanthophylls (Briantais et al. 1980; Demmig-Adams 1990). The most immediate effect of NPQ is to maintain the redox poise of the

Abbreviations and symbols: Anth = antheraxanthin; Chl = chlorophyll; F_{max} = maximum fluorescence yield (all PSII traps closed) in fully dark-adapted state; F'_m = maximum fluorescence yield in the light-adapted state; F_o = minimum fluorescence yield (all PSII traps open) in fully dark-adapted state; F'_o = minimum fluorescence yield in the light-adapted state; F_s = steady-state fluorescence yield; $F'_v = (F'_m - F'_o)$; LHCII = light-harvesting complex of PSII consisting of the Lhcb1, Lhcb2, Lhcb3, Lhcb4, Lhcb5, Lhcb6 proteins; NPQ = nonphotochemical quenching ($F_{max}/F'_m - 1$); Q_A = primary quinone electron acceptor of PSII; qN = nonphotochemical quenching coefficient $[(F_{max} - F'_m)/(F_{max} - F'_o)]$; qP = photochemical quenching coefficient $[(F'_m - F_s)/(F'_m - F'_o)]$; Viol = violaxanthin; WT = wild type; Φ_{II} = photochemical yield of PSII $[(F'_m - F_s)/F'_m]$; Θ = light-stress response $[1 - F_s(\text{air})/F_s(5\%\ O_2)]$; Zea = zeaxanthin

Correspondence to: R.B. Peterson;
E-mail: Richard.Peterson@po.state.ct.us;
Fax: 1 (203) 974 8502;

photosynthetic electron transport chain at a more oxidized level than it would be if the photoprotective response were absent. Although increases in NPQ result in reduced light-use efficiency for photosynthesis, associated photodamage is mitigated, enabling rapid re-establishment of high quantum yield if irradiance falls to limiting levels.

One powerful way to elucidate the mechanism and regulation of NPQ is to identify genes controlling this phenomenon. We hypothesized that some genes required for induction of NPQ would direct no vital function in the absence of excessive illumination. Consequently, growth and light utilization efficiency (as revealed by fluorescence yield measurements) for an NPQ-deficient mutant should be indistinguishable from that of the wild type (WT) at low photon flux rates. This has been shown for NPQ-deficient mutants of *Chlamydomonas reinhardtii* and *Arabidopsis thaliana* that possess lesions in the xanthophyll cycle (Niyogi et al. 1997, 1998). Since PSII reaction centers compete effectively with fluorescence for excitation in low light, the steady-state fluorescence yield (F_s) for NPQ-deficient mutants would also be low and similar to that of the WT. However, in normal chloroplasts a transition from conditions of light limitation to light stress imposed by reducing the availability of terminal acceptors for photosynthetic electron transport increases the rate constant for thermal dissipation of energy in the PSII antennae (Krause and Weis 1991). This response essentially offsets the decline in energy use by PSII photochemistry so that F_s is not affected appreciably. In contrast, the density of excitation in the antenna system of an NPQ-deficient mutant should increase after this transition due to a lower rate constant for heat production causing increased energy flow to fluorescence. Hence, screening of mutagenized populations of *Arabidopsis* for increases in F_s accompanying abrupt shifts in gas-phase composition could identify NPQ-deficient variants.

Some NPQ mutants may exhibit reduced photosynthetic pigment levels. A pale phenotype could result from enhanced photooxidative destruction of pigments due to loss of photoprotective thermal dissipation. In this study we tested 62 yellow-green mutant lines originally isolated in Dr. Kenneth Feldmann's laboratory (Feldmann 1991) for reduced NPQ capacity using fluorescence imaging. One line carried a single nuclear mutation that resulted in a substantial loss in NPQ capacity although it possessed normal capacity for the reversible conversion of violaxanthin to antheraxanthin and zeaxanthin under conditions of light stress.

Materials and methods

Plant material and growth conditions. Sixty-two lines of *Arabidopsis thaliana* (L.) Heynh. reported to segregate a yellow-green phenotype were obtained from the Arabidopsis Biological Resource Center (ABRC) at Ohio State University. These mutant lines (ecotype Wassilewskija) were originally created by *Agrobacterium* seed transformation and deposited in the collection by Dr. Kenneth Feldmann (Feldmann 1991). Seeds were placed on half-strength Murashige-Skoog medium (no sucrose) supplemented with 1.4% agar in 10-cm-diameter Petri plates. The plates were maintained at 5 °C in the dark for 2–3 d to enhance germination frequency. Plates were then placed in a growth chamber with a 12 h day:12 h night regime with corresponding temperatures of 23 °C:20 °C. An irradiance of 120 μmol photons m^{-2} s^{-1} was provided by a combination of Cool White and incandescent lamps. Growth to maturity followed transplantation of seedlings to a commercial potting soil mixture. Where indicated, excised leaves were floated on a 10.0 mM solution of DTT (Sigma, St. Louis, Mo., USA). The leaves were incubated in air and ambient light for 30 min followed by at least 1 h of darkness. Control leaves were subjected to the same treatment but DTT was omitted.

Screening for NPQ mutants. Steady-state fluorescence images were captured using a video analysis system described previously (Peterson and Aylor 1995). Fluorescence excitation was provided as white light using a Schott KL1500 Cold Light Source equipped with a bifurcated light guide. Lenses fitted with heat-reflecting mirrors (Optical Coatings Laboratory, Santa Rosa, Calif., USA) to exclude wavelengths >700 nm were mounted on the ends of the light guide and provided a uniform illumination at an irradiance of 200 μmol photons m^{-2} s^{-1}. A Schott RG9 transmission filter (3 mm thick) was placed in front of the camera lens to block wavelengths <700 nm.

Approximately 50 seeds were distributed within an area of 15 cm^2 on a Petri plate as described above. After 4–6 d of growth pre-illuminated plates were removed from the growth chamber and immediately covered with a Plexiglas cover fitted with ports to allow gassing of the enclosed volume. The plate was flushed first with humidified air at a flow rate of 500 ml min^{-1} for 2 min followed by capture of a steady-state fluorescence image. The plate was then flushed for 2 min with CO_2-free 5% (v/v) O_2, followed by capture of a second image. The raw images were processed using software to compensate for pixel nonlinearity. An image representing the change in steady-state fluorescence emission accompanying the shift in gas phase from air to 5% O_2 (**Θ**) was computed pixel-by-pixel from the successive steady-state fluorescence images as $[1 - F_s(\text{air})/F_s(5\%\ O_2)]$. A total of approximately 100 seedlings per line was examined.

Pulse-modulated-fluorescence measurements. The Chlorophyll Fluorescence System (H. Walz, Effeltrich, Germany) was employed for measurements of fluorescence yield (Peterson 1991). Continuous actinic illumination was directed to the sample via the same fiberoptic system that carried the measuring beam. For seedlings at the cotyledon stage of development the Petri plate was covered with Plexiglas containing a port that allowed positioning of the measuring probe to within approx. 5 mm of the sample. Fluorescence-yield measurement in excised true leaves was performed using a Leaf Section Chamber (Analytical Development Co., Hoddesdon, UK). A filter-paper disc placed on the floor of the chamber was covered with a thin layer of distilled H_2O. The leaf rested on a thermistor probe protruding from the chamber floor so that only the cut end was immersed in the H_2O. The chamber volume was flushed with either air or 5% O_2 as described above. A thermostatted circulator connected to the chamber water jacket maintained leaf temperature at 23 °C. The fiberoptic illuminator was positioned outside the chamber window. Saturating pulses of white light (6000 μmol photons m^{-2} s^{-1} for 0.7 s) were provided by a separate Schott KL1500 light source. The modulation frequency of the measuring beam was 1.6 kHz for measurements of minimum fluorescence yields in the fully dark-adapted (F_o) and light-adapted (F_o') states. Weak far red (720 nm) illumination was provided during F_o' measurements to ensure that all PSII traps were open. The modulation frequency under all other conditions was 100 kHz. Fluorescence nomenclature and formulae (i.e. NPQ, F_v'/F_m', Φ_{II}, qN, qP) conform to definitions described previously (Genty et al. 1989; van Kooten and Snel 1990).

Analysis of pigments and thylakoids. Leaf samples were frozen in liquid N_2 and stored at −70 °C. Ground samples were

extracted two or three times with cold 85% acetone. Determination of total chlorophyll (Chl) in acetone extracts was performed using the extinction coefficients of Lichtenthaler (1987). Separation of pigments in extract supernatants was performed by reverse-phase HPLC on a Spherasorb S5 ODS2 column (25 cm long, 4.6 mm i.d.; Phase Separations, Norwalk, Conn., USA). A chromatographic separation began with 20 min of solvent A (acetonitrile: ethyl acetate: H_2O: 0.2 M Tris pH 8.0, 75:20:5:1, by vol.) at a flow rate of 0.9 ml min^{-1} to elute Chl *b* and the xanthophylls neoxanthin (Neo), violaxanthin (Viol), antheraxanthin (Anth), lutein (Lut) and zeaxanthin (Zea). A linear gradient from solvent A to 30% solvent A/70% solvent B (acetonitrile: ethyl acetate, 4:1, v/v) was developed over 2 min at 1.0 ml min^{-1} (elution of Chl *a*) and maintained at the final composition for 15 min (elution of β-carotene). The column was re-equilibrated to starting conditions by imposing a linear gradient to 100% solvent A over 2 min and flushing with solvent A for 40 min. Eluting pigment peaks were quantitated based on absorbance at 440 nm. Factors to convert integrated absorbance of Chl *a*, Chl *b*, Lut, Zea, and β-carotene peaks to mass were obtained by use of standards (Sigma; Atomergic Chemicals, Farmingdale, N.Y., USA) and published extinction coefficients (Havir et al. 1997). The conversion factor for Viol was obtained from purified Viol as described by Havir et al. (1997) and that of Anth was estimated as the mean of the coefficients for Viol and Zea. The extinction coefficient for Neo was based on the value for Viol times the Neo/Viol ratio of Färber et al. (1997). The degree of de-epoxidation of xanthophyll cycle intermediates was calculated as (Zea + 0.5 · Anth)/(Viol + Anth + Zea).

Thylakoid membranes were prepared and SDS-PAGE electrophoresis was performed using the methods of Peter and Thornber (1991). Separated proteins were transferred to a polyvinylidenedifluoride membrane (Millipore Corp) and probed with preparations of antibodies to the light-harvesting complex of PSII (LHCII). The first preparation contained antibodies against the Lhcb1 and Lhcb2 proteins and was applied at a dilution of $1{:}10^4$. Individual preparations containing antibodies against Lhcb2, Lhcb3, Lhcb4, Lhcb5, and Lhcb6 were used at a dilution of $1{:}10^2$. Antigen:antibody complexes were visualized using the alkaline-phosphatase reaction.

Genetics and mapping. Pollen from a putatively homozygous, NPQ-deficient line was used in an outcross to ecotype Columbia. The resulting F_1 plants were allowed to self-fertilize producing a F_2 seed population. The distribution of Θ was assessed in F_3 progenies of > 50 seedlings derived by self-fertilization of each individual F_2 plant. The parental lines were included as controls. The F_2 lines were classified as segregating uniformly normal (i.e. WT), uniformly mutant, or a mixture of normal and mutant progeny. Genomic DNA samples were prepared from the F_3 progeny populations and tested for presence of microsatellite and simple sequence length polymorphism marker alleles using the polymerase chain reaction (Bell and Ecker 1994).

Results

Application of fluorescence methods to detect and characterize an NPQ-deficient mutant. Fluorescence imaging is an efficient means of screening seedling populations for NPQ-deficient variants (Niyogi et al. 1997). Pulse-modulation fluorimetry is incapable of resolving spatial differences but does provide accurate verification and detailed information concerning how light energy is used by PSII (van Kooten and Snel 1990). Figure 1 shows images of Θ for WT *A. thaliana* and for a homozygous population of seedlings derived from the only line among the original 62 mutant lines tested that segregated variants exhibiting diminished NPQ capacity (ABRC stock CS2767, Feldmann line 3116). We hereafter refer to this mutation as *lsr1* (*light stress response* deficient). Shown also in the figure are typical pulse-modulated-fluorescence induction transients for WT and mutant. Steady-state levels of NPQ attained after several minutes of illumination in air were low in air for both WT and mutant as indicated by relatively high readings for F'_m (maximum fluorescence yield in the light-adapted state). However, after a transition to 5% O_2 the magnitude of F'_m declined in both WT and mutant but to a relatively lesser extent in the latter. Also, the steady-state F_s in 5% O_2 increased significantly compared to that in air for the mutant but was scarcely affected for WT. Consistent with these changes in F_s, the mean value of Θ as indicated in the images was higher for the mutant compared to WT. We note that mean values of Θ were somewhat lower in the images due to the slightly higher irradiance employed compared to the pulse-modulated-fluorescence measurements. However, under identical conditions mean values of Θ were always higher for $Lsr1^-$ than for WT.

Additional properties associated with illumination under air or 5% O_2 are compared in Table 1. Consistent with the results shown in Fig. 1, the magnitude of F_s (normalized to the corresponding F_{max}) was highest in 5% O_2 for the mutant but was substantially lower and not appreciably affected by gas-phase composition for WT or by genotype in air. The higher value of Θ for $Lsr1^-$ is attributable to these differences in F_s. The alternate indicators of reversible energy dissipation, nonphotochemical quenching (NPQ = $F_{max}/F'_m - 1$) and the nonphotochemical quenching coefficient [qN = $(F_{max} - F'_m)/(F_{max} - F'_o)$], were slightly lower in the mutant compared to WT under unstressed conditions (i.e. air). However, reduced capacity for energy dissipation in the mutant was pronounced when leaves were subjected to light stress (i.e. 5% O_2). Under the latter conditions, NPQ and qN levels were 59% and 28% lower, respectively, in the mutant relative to WT. The magnitudes of NPQ and light-capture efficiency by PSII (F'_v/F'_m) are inversely (albeit nonlinearly) related. Hence, the change from air to 5% O_2 resulted in a 33% versus 10% decline in F'_v/F'_m for WT and mutant, respectively. The product of F'_v/F'_m and fraction of open PSII traps (qP, photochemical quenching coefficient) has been proposed as a measure of quantum efficiency of light use for linear photosynthetic electron transport (Φ_{II}; Genty et al. 1989]. Levels of qP and Φ_{II} declined in both WT and mutant in response to restricted availability of electron acceptors in 5% O_2 compared to air (Table 1). However, Φ_{II} was significantly higher in 5% O_2 for the mutant compared to WT indicating that reduced capacity for thermal dissipation was balanced, in part, by increased energy use for electron transport. Table 1 also shows that the increase in light stress is accompanied by a significant increase in de-epoxidation state of xanthophyll-cycle intermediates. Further comparisons of pigment content are shown in Table 2. In fully dark-adapted leaves, the xanthophyll-cycle intermediates are nearly completely epoxidized with Anth and Zea levels generally below the detection limit.

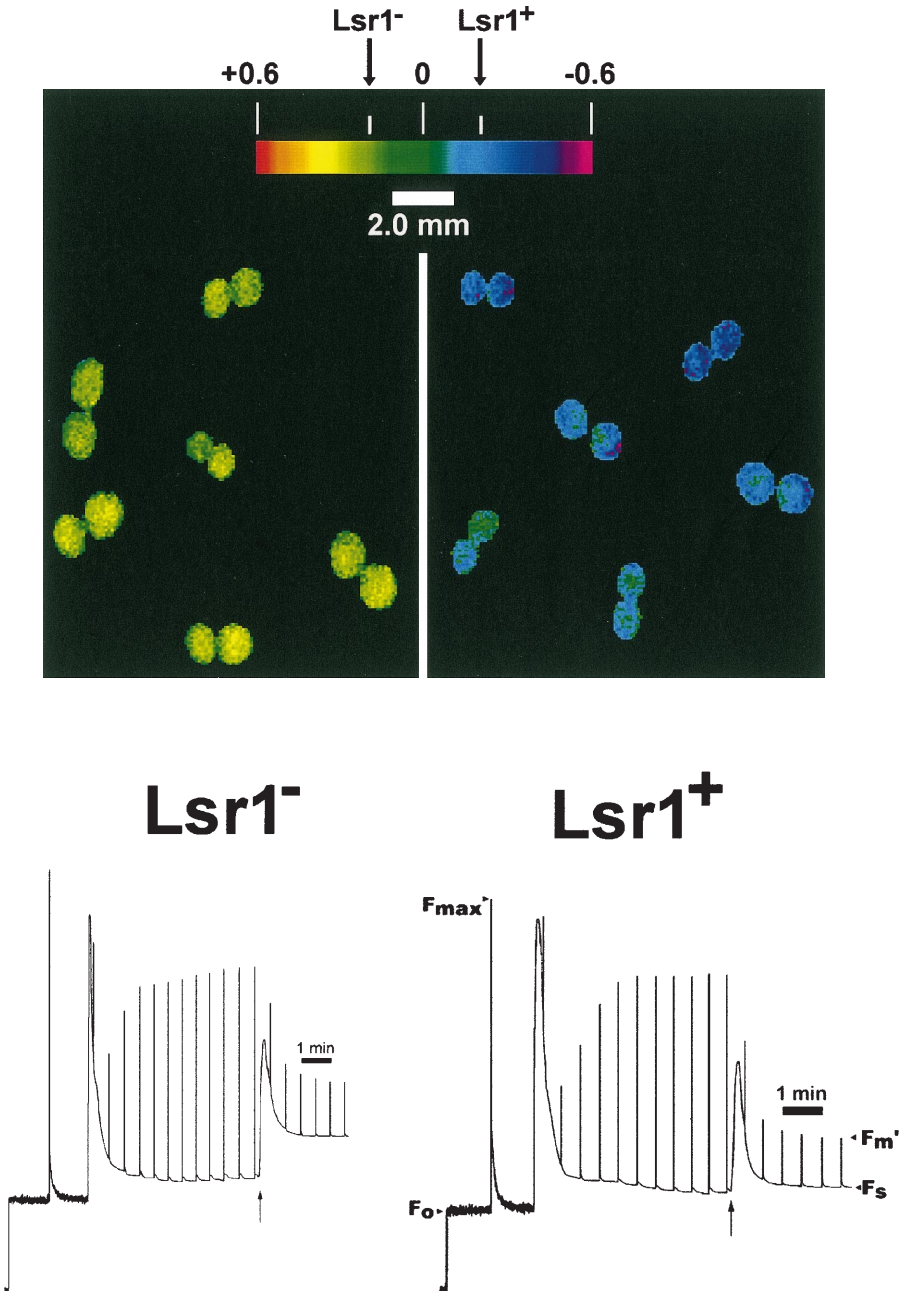

Fig. 1. Illustration of the NPQ-deficient phenotype (Lsr1$^-$) in comparison to WT (Lsr1$^+$) *Arabidopsis thaliana*, based on imaging of steady-state fluorescence emission and application of pulse-modulated-fluorescence yield measurements using seedling populations at the cotyledonary stage of development. False-color images show the distribution of Θ computed from successive images captured under conditions of air and CO_2-free 5% (v/v) O_2 (see *Materials and methods*). Mean values (±SD) of Θ are indicated on the colored scale bar and correspond to −0.200 ± 0.123 and 0.186 ± 0.076 for WT and mutant, respectively. The *white horizontal bar* denotes size. Fluorescence yield induction transients were obtained for material that had been dark-adapted for at least 20 min. Critical fluorescence yield levels are labelled for the WT trace. The rise in signal to F_o accompanied switching on of the measuring beam. A saturating pulse was applied to measure the level of F_{max}, the maximum fluorescence yield in the fully dark-adapted state. Continuous illumination (120 μmol photons m^{-2} s^{-1}) was supplied 1 min later causing the large initial excursion in F_s. Saturating pulses were superimposed at intervals of 30 s. The gas phase was switched from air to CO_2-free 5% O_2 at the point indicated (↑) and recording terminated once a steady state had been achieved. See text for further discussion

Table 2 shows also that total Chl levels per unit leaf area are essentially identical in WT and mutant, and that levels of individual pigments and maximum quantum efficiency (F_v/F_{max}) were not significantly affected by genotype.

The results of Fig. 1 and Table 1 indicate that overall light utilization efficiency for photosynthesis was comparatively high for both WT and Lsr1$^-$ under conditions simulating those used to grow the seedlings (i.e. air, 120 μmol photons m^{-2} s^{-1}, 23 °C). We observed that the majority (55) of the original mutant lines tested did not segregate yellow-green progeny. Lack of expression of a pale phenotype probably indicates that our growth conditions contrasted with those employed in the initial screening (Feldmann 1991). Nevertheless, expression of a reduced-pigment phenotype is not a prerequisite for valid screening for associated NPQ deficiency. Of the seven lines that did segregate pale individuals there was a strong correlation between pigment loss and high Chl fluorescence yield in air and low light. This is a characteristic of lesions in the linear photosynthetic electron transport chain from H_2O to CO_2 (Meurer et al. 1996). Since such mutations are likely to be pleiotropic, their relevance to regulation of NPQ is questionable and they were not examined further.

Figure 2A compares fluorescence induction kinetics for WT and Lsr1$^-$ in air. Re-illumination following several hours of darkness resulted in a rapid increase in NPQ that relaxed in 2 min. The extent of the initial rise in NPQ was reduced significantly in the mutant. The PSII acceptor Q_A showed a high degree of reduction (i.e. low qP) at 10 s following re-illumination (Fig. 2A). The

Table 1. Light utilization properties of WT and Lsr1$^-$ *Arabidopsis* measured under steady-state conditions in the absence (air) and presence (CO_2-free 5% O_2) of light stress. The irradiance was 120 μmol photons m^{-2} s^{-1} and the temperature was 23 °C. Results shown are means of three to six replicates (±SE). See text for definitions of parameters

Parameter	WT	Lsr1$^-$
F_s/F_{max}		
Air	0.295 ± 0.008	0.316 ± 0.010
5% O_2	0.281 ± 0.007	0.457 ± 0.011
Θ	−0.031 ± 0.014	0.294 ± 0.010
NPQ		
Air	0.682 ± 0.064	0.530 ± 0.054
5% O_2	2.323 ± 0.040	0.961 ± 0.040
qN		
Air	0.489 ± 0.029	0.419 ± 0.028
5% O_2	0.833 ± 0.004	0.597 ± 0.013
F_v'/F_m'		
Air	0.696 ± 0.011	0.720 ± 0.008
5% O_2	0.465 ± 0.005	0.647 ± 0.008
qP		
Air	0.723 ± 0.026	0.719 ± 0.021
5% O_2	0.144 ± 0.040	0.160 ± 0.008
Φ_{II}		
Air	0.504 ± 0.024	0.518 ± 0.019
5% O_2	0.067 ± 0.019	0.103 ± 0.004
Xanthophyll de-epoxidation (%)		
Air	16.0 ± 4.0	8.4 ± 0.9
5% O_2	43.8 ± 13.5	35.6 ± 7.4

subsequent rises in qP (Fig. 2A) and Φ_{II} (Fig. 2B) for WT and mutant were similar and lagged significantly behind the respective increases in NPQ.

Inheritance and mapping of lsr1. For 59 F_2 lines the frequency of occurrence of exclusively WT: mixture of WT and mutant: exclusively mutant phenotypes in the respective F_3 progenies was 13:31:15 (see *Materials and methods*). These results are consistent with segregation of *lsr1* as a single nuclear trait and allow assignment of the genotypes of the respective F_2 classes as *LSR1 LSR1*, *LSR1 lsr1*, and *lsr1 lsr1*. Figure 3 compares steady-state NPQ for WT leaves and leaves either homozygous or heterozygous for the Lsr1$^-$ mutation under light-limited (air) and light-stressed (5% O_2) conditions. Surprisingly, the NPQ level observed in 5% O_2 for the heterozygote was not significantly different from that of the homozygote. We also observed

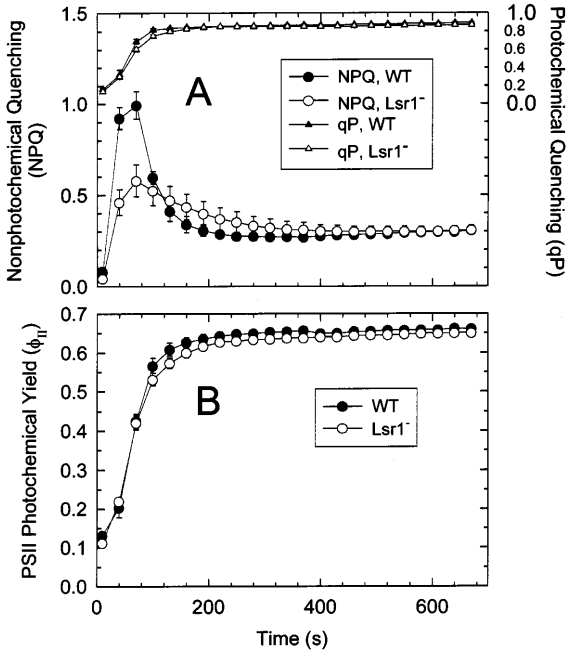

Fig. 2A,B. Induction of NPQ and qP (**A**) and Φ_{II} (**B**) in excised true leaves from WT and Lsr1$^-$ *Arabidopsis*. Leaf samples were darkened for 3 h prior to illumination at time zero with 120 μmol photons m^{-2} s^{-1} in air. Measurements of NPQ commenced 10 s after the start of illumination and were thereafter acquired at 30-s intervals. Each point is a mean (±SE) based on measurements with three replicate leaf samples

Table 2. Pigment composition and maximum quantum yield (F_v/F_{max}) of dark-adapted leaf samples of WT and Lsr1$^-$*Arabidopsis*. Excised leaves were floated on distilled H_2O in total darkness for 3 h prior to measurement. Total Chl in leaf discs was determined spectrophotometrically (see *Materials and methods*). Individual pigments were determined by HPLC. Mean values based on at least six replicate leaf samples (±SE). n.d., not detected

Parameter	WT	Lsr1$^-$
Total Chl (mg/m^2)	174.7 ± 9.6	174.5 ± 1.6
Pigment (mmol/mol Chl *a*)		
Neoaxanthin	46.0 ± 2.7	41.2 ± 2.8
Violaxanthin	37.4 ± 2.3	34.0 ± 1.4
Antheraxanthin	n.d.	0.3 ± 0.2
Lutein	130.8 ± 7.2	121.5 ± 4.5
Zeaxanthin	n.d.	n.d.
Chl *b*	361.8 ± 8.0	357.9 ± 8.0
β-Carotene	27.7 ± 2.8	30.6 ± 2.1
F_v/F_{max}	0.800 ± 0.003	0.802 ± 0.002

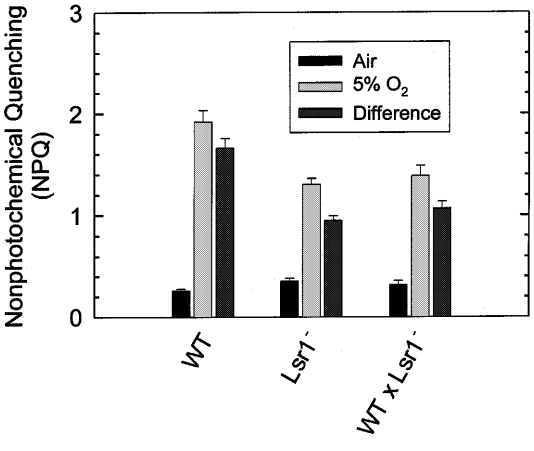

Fig. 3. Comparison of NPQ in air and 5% O_2 for leaves of WT *Arabidopsis*, mutant Lsr1, and an F_1 plant heterozygous for the mutation (WT × Lsr1$^-$). The irradiance was 120 μmol photons m^{-2} s^{-1}. Mean values were based on four replicate determinations

Table 3. Chi Square (χ^2) test for linkage between chromosome 1 molecular markers and *lsr1*. The NPQ genotype was determined for each *Arabidopsis* plant of an F_2 outcross population as described in the text. Only homozygous F_2 plants (i.e. *LSR1 LSR1* and *lsr1 lsr1*) were tested (total of 56 chromosomes). Testing for the presence of alleles of molecular markers corresponding to Wassilewskija and Columbia parental lines was performed using genomic DNA as described in *Materials and methods*. Recombination frequency is the number of chromosomes exhibiting a crossover event between the molecular marker and *lsr1* locus divided by 56. NS, not significant ($P > 0.5$); *$P < 0.005$

Marker	Recombination frequency %	χ^2
nga63	46.4	1.72 (NS)
nga248	21.4	18.86*
nga280	19.6	21.00*
T27K12	8.9	38.14*

in images of Θ that only about 25% of the progeny derived from plants heterozygous for *lsr1* exhibited signals clearly typical of WT seedlings (not shown). Many seedlings appeared to possess a signal that was intermediate to that of WT and the *lsr1* homozygote. Despite some variability in expression of the NPQ-deficient phenotype by *LSR1 lsr1* heterozygotes we conclude that *lsr1* is best described as semidominant. Figure 3 also shows the difference [NPQ (5% O_2) − NPQ (air)] which is a measure of the increase in the rate constant for thermal dissipation relative to that of the fully dark-adapted state.

Table 3 shows linkage data for *lsr1* and three molecular markers on chromosome 1. The mutation shows significant linkage to markers nga248, T27K12, and nga280 all located near the middle of the chromosome. The distribution of these markers in relation to the approximate location of *lsr1* is shown in Fig. 4. Note that the microsatellite marker nga63 located approximately 10 centimorgans (cM) from the end of chromosome 1 is unlinked to the *lsr1* locus (Table 3). Southern hybridization using the pYU179 plasmid (which carries the 35 S/Npt2/NOS insert) as a probe of genomic DNAs obtained from an F_2 population failed to demonstrate co-osegregation of a T-DNA insert with *lsr1*. Hence, *lsr1* is probably an example of mutagenesis associated with an abortive *Agrobacterium* gene transfer event.

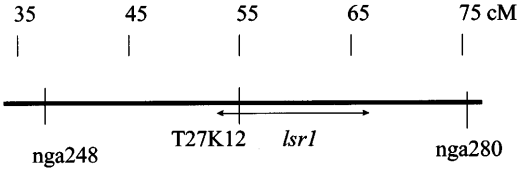

Fig. 4. Distribution of molecular markers nga248, T27K12, and nga280 in relation to *lsr1* on chromosome 1. Positions of the molecular markers are based on the map of Meinke et al. (1998). The limits of the interval that includes *lsr1* are shown by the *double arrow* and are based on analysis of the linkage data in Table 3 (Lander et al. 1987)

Lsr1⁻ in relation to the xanthophyll cycle and LHCII composition. Figure 5 shows effects of irradiance on NPQ (panel A) and associated changes in steady-state levels of xanthophyll-cycle intermediates (panel B). The differences in NPQ capacity in WT and Lsr1⁻ increased progressively with increasing irradiance and each could be fitted to a hyperbola (see legend to Fig. 5). These fits indicated that the difference in NPQ level could not be overcome at infinite irradiance. Consequently, *lsr1* results in a 54% loss of maximum NPQ capacity as well as a shift of the irradiance response to lower light levels as indicated by the lower $I_{0.5}$ value. In contrast to the effect of irradiance on NPQ, changes in levels of the xanthophyll-cycle intermediates Viol, Anth, and Zea with increasing irradiance were the same for WT and

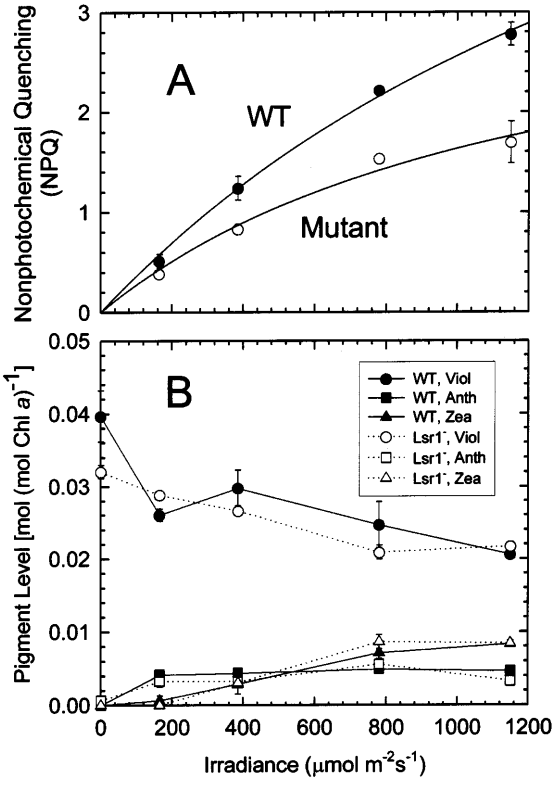

Fig. 5A,B. Effect of irradiance on NPQ (**A**) and associated levels of xanthophyll-cycle intermediates (**B**) for true leaves of WT and Lsr1⁻ *Arabidopsis*. Fluorescence yield levels were recorded after 15–20 min at each indicated irradiance and followed immediately by transfer of the leaf sample to liquid N_2. The solid lines in **A** are hyperbolic fits to the data according to $P \cdot I/(I_{0.5} + I)$ where I is the irradiance, P is the maximum level of NPQ, and $I_{0.5}$ is the irradiance associated with half-maximal NPQ. Maximum likelihood values of P and $I_{0.5}$ were estimated by reiterative substitution to obtain a minimum sum of squares for predicted versus observed NPQ. Coefficients of determination for the fits were 0.98 and 0.91 for WT and Lsr1⁻, respectively (10 degrees of freedom, $P < 0.01$). The optimum values of P (±SE) were 7.8 ± 0.6 and 3.6 ± 0.5 for WT and mutant, respectively. The respective values of $I_{0.5}$ (μmol m^{-2} s^{-1}) for WT and mutant were 2040 ± 225 and 1205 ± 330. The pigment data of **B** were subjected to two-way ANOVA that indicated that irradiance was the only significant (i.e. $P < 0.05$) source of variation for the individual metabolites. Neither irradiance nor genotype was a significant source with respect to the sum (Viol + Anth + Zea) [$P > 0.10$]. Each point is a mean of three replicates

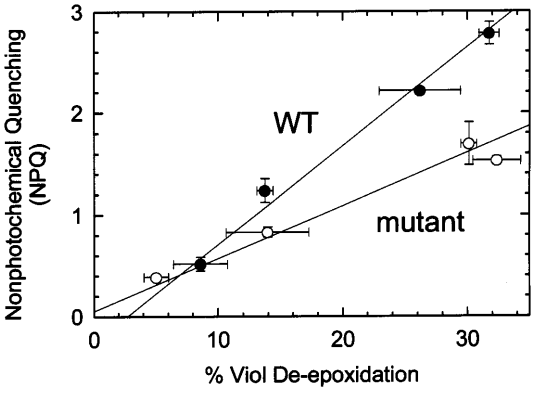

Fig. 6. Relationship between the extent of violaxanthin de-epoxidation and NPQ for WT and Lsr1$^-$ *Arabidopsis*. The data are from Fig. 5 and plotted as the respective means at each irradiance. The solid lines are linear regression fits to the unaveraged data. The coefficients of determination were 0.87 and 0.82 for WT and Lsr1$^-$, respectively ($P < 0.01$). The slopes (±SE) were $9.71 \times 10^{-2} \pm 1.18 \times 10^{-2}$ for WT and $5.19 \times 10^{-2} \pm 7.63 \times 10^{-3}$ for Lsr1$^-$

mutant when normalized to the corresponding Chl *a* levels (Fig. 5B). The decline in Viol with increasing irradiance was balanced by increases in Anth and Zea so that the sum (Viol + Anth + Zea) was unaffected by either irradiance or genotype as shown by two-way analysis of variance (ANOVA; see legend of Fig. 5).

A comparison of the extent of xanthophyll-cycle de-epoxidation to NPQ based on the results of Fig. 5 indicates linear dependencies extrapolating to near the origin for both WT and mutant (Fig. 6). However, the slopes of the regression lines are significantly different, indicating that for a given degree of xanthophyll de-epoxidation less NPQ develops in the mutant compared to the WT. We examined the relationship between NPQ and xanthophyll de-epoxidation further by treating WT and mutant leaves with DTT, an inhibitor of Viol de-epoxidase (Demmig-Adams et al. 1990; Havir et al. 1997). Figure 7 shows that DTT treatment profoundly affects induction of NPQ in strong light for both WT and Lsr1$^-$. A rapid increase in NPQ occurred during the initial 2 min of illumination and was followed by a slow increase in untreated leaves. The extent of development of NPQ was approx. 40% less in the mutant compared to the WT at the end of the experiment. Treatment with DTT sharply reduced the amplitude of the initial rapid increase in NPQ but had little effect on the kinetics of the slow phase of WT and mutant. Hence, mutant leaves exhibited a relatively smaller sensitivity to DTT treatment. The results indicate that the effect of *lsr1* is to specifically diminish (Zea + H^+)-dependent quenching (dashed lines Fig. 7A,B). At the DTT concentration employed (10 mM), inhibition of Viol de-epoxidation was >95% (see legend to Fig. 7). We observed an inhibition of Φ_{II} for both WT and mutant that depended on the length of time of dark preincubation with DTT. This could be due to inhibition of Mehler reaction activity, specifically ascorbate peroxidase, by DTT (Neubauer 1993). However, lower values of Φ_{II} were not associated with correspondingly lower NPQ levels

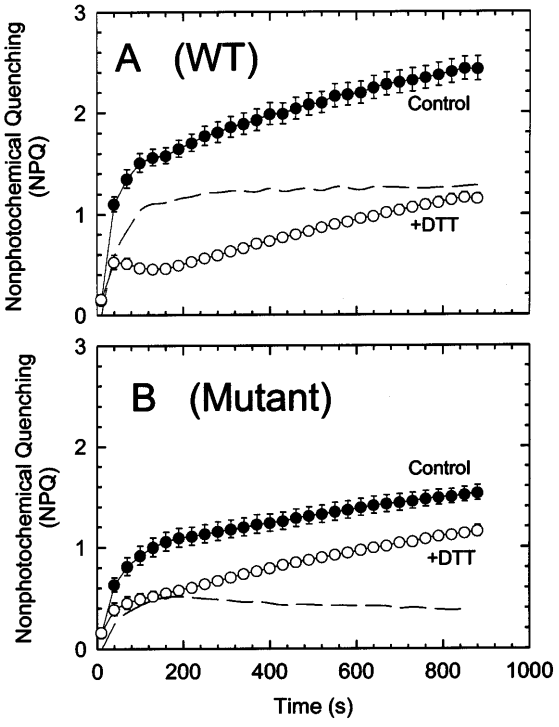

Fig. 7A,B. Effects of DTT on induction of NPQ in WT (**A**) and Lsr1$^-$ (**B**) *Arabidopsis*. At time zero, pre-darkened leaves were illuminated at an irradiance of 1450 μmol photons m^{-2} s^{-1}. Saturating pulses were delivered at time intervals described in Fig. 2. Each point is a mean (±SE) of six determinations. The pigment composition of samples was analyzed at the end of the experiment. The degree of de-epoxidation of Viol was 46.0 ± 4.5% and 43.8 ± 4.1%, respectively, for WT and mutant controls. Treatment with DTT reduced Viol de-epoxidation to 1.3 ± 0.8% and 4.0 ± 1.3% for WT and Lsr1$^-$, respectively. The *dashed lines* represent Zea-dependent NPQ calculated as the difference between the control and +DTT curves

for DTT-treated leaves of either line based on linear regression ($P > 0.15$). Hence, development of NPQ was not limited by electron transport rate in these experiments.

A central feature of ΔpH-dependent thermal dissipation is quenching of fluorescence yield when reaction centers are closed (F'_m) or open (F'_o) although this is more pronounced with regard to F'_m (Peterson 1991). Figure 8 shows that suppression of F'_o increased linearly with NPQ for WT. Corresponding measurements for Lsr1$^-$ were not significantly different than WT for the three lower irradiance levels but deviated significantly at the highest irradiance.

We sought evidence for gross changes in LHCII integrity in Lsr1$^-$. The SDS-PAGE (Fig. 9A) analysis of thylakoid membranes showed depletion of an approx. 53 kDa band for Lsr1$^-$. However, this feature was not observed in all preparations. No consistent genotype-specific changes in protein composition occurred among several thylakoid preparations from WT and Lsr1$^-$. Likewise, no difference in protein level or electrophoretic mobility was detected for the trimeric peripheral-antennae proteins (Lhcb1–3) or monomeric inner-antennae proteins (Lhcb4–6) of PSII based on Western blots (Fig. 9B).

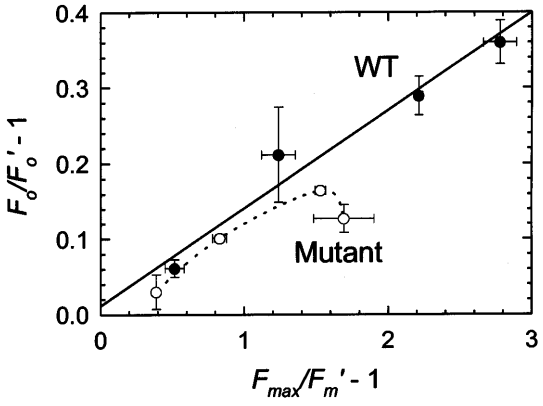

Fig. 8. Comparisons of the degree of suppression of "dark level" fluorescence (F_o' versus F_o) and corresponding NPQ levels for WT and Lsr1$^-$ *Arabidopsis*. The results were obtained from the experiment of Fig. 5 and the means (±SE) correspond to the four irradiance levels employed

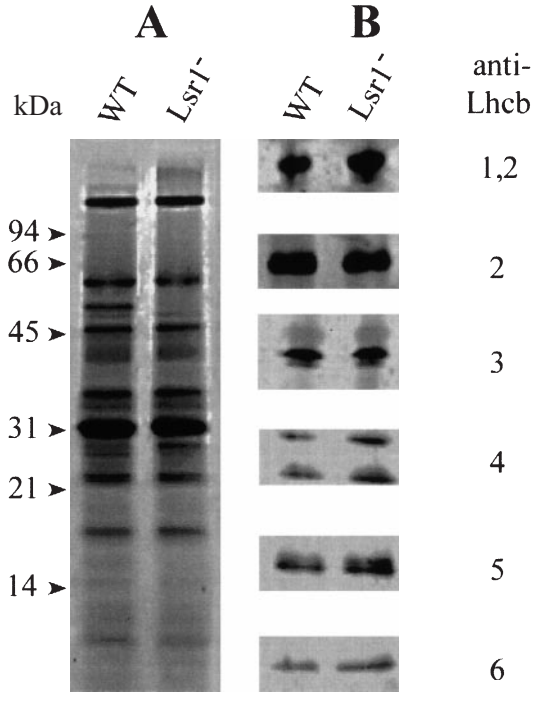

Fig. 9A,B. Analaysis of thylakoids by SDS-PAGE (**A**) and immunoblots (**B**) showing levels of PSII light-harvesting Chl *a*/*b* proteins for WT and Lsr1$^-$ *Arabidopsis*. The amount of total Chl applied for each lane was 20.0 μg for the protein gels and 3.0 μg for the immunoblots. Note that the upper band observed with the anti-Lhcb4 antibody preparation corresponds to Lhcb4 (Judy Brusslan, personal communication). See *Materials and methods* for further information

Discussion

The *A. thaliana* line Lsr1$^-$ displays essentially identical pigment composition (Table 2), growth, and appearance compared to WT under the comparatively moderate growth conditions employed in this study. In contrast, Lsr1$^-$ is less efficient than WT in responding to light stress as evidenced by a 54% lower total NPQ capacity in saturating light (Fig. 5A). This loss is associated with an attenuated initial rise in NPQ following re-illumination of pre-darkened leaf material (Fig. 2A). The rise in NPQ precedes oxidation of Q_A^- by PSI as indicated by increasing qP which, in turn, coincides with the induction of linear electron transport (Fig. 2B). These features have been interpreted in terms of a delay in initiation of NADPH- and ATP-utilizing Calvin cycle reactions following re-illumination so that reduced electron transport components and lumenal H^+ ions transiently accumulate (Quick and Horton 1984). Hence, the initial excursion in NPQ is associated with changes in ΔpH, as supported by parallel changes in membrane energization occurring on a similar time scale (Sivak et al. 1985). The results indicate that reduced NPQ capacity in Lsr1$^-$ is associated with partial loss of a ΔpH-dependent phase possessing rapid onset and relaxation kinetics often referred to as qE (Horton et al. 1996).

We approach the question of the physiological basis for the NPQ-deficient phenotype by sequentially evaluating evidence concerning associated effects on: (i) the xanthophyll cycle, (ii) ΔpH formation, and (iii) properties of the LHCII. A large volume of evidence points to involvement of Zea (and Anth) in the mechanism of NPQ (Demmig-Adams 1990; Gilmore and Yamamoto 1993; Horton et al. 1996). Studies with mutants of *Chlamydomonas reinhardtii* and *A. thaliana* in which Viol de-epoxidase or Zea epoxidase were absent have confirmed this (Niyogi et al. 1997, 1998). The apparently normal capacity for reversible accumulation of Zea and Anth in Lsr1$^-$ (Fig. 5B) distinguishes this phenotype from previously described xanthophyll-cycle mutants. A phenotype apparently similar to Lsr1$^-$ was reported recently for the *npq4* mutation of *A. thaliana* (Björkman and Niyogi 1998). Since *npq4* maps to the same region of chromosome 1 as *lsr1* (Fig. 4) it is possible that these mutations are allelic (K.K. Niyogi, personal communication).

It is well established that induction of NPQ in chloroplasts is dependent upon formation of a transthylakoidal ΔpH (Horton et al. 1996). Nuclear mutations that disrupt linear photosynthetic electron transport from H_2O to CO_2 also inhibit H^+ translocation. These lesions are generally associated with reduced pigment levels and an impairment (if not total loss) in capacity for photoautotrophic growth (Meurer et al. 1996). Fluorescence induction (Figs. 1 and 2B) and steady-state parameters relating to light-use efficiency in PSII in air (i.e. NPQ, qN, qP, F_v'/F_m', and Φ_{II}, see Table 1) are similar in Lsr1$^-$ and WT. Hence, electron transport and associated processes in Lsr1$^-$ are not affected appreciably under light-limited conditions that simulate those used to grow the plants. However, the results provide evidence that ΔpH formation is also identical in WT and Lsr1$^-$ when light stress is imposed. The conversion of Viol to Anth and Zea is catalyzed by Viol de-epoxidase possessing a pH optimum of 5 and localized on the lumen-facing side of the thylakoid membrane (Siefermann and Yamamoto 1975; Havir et al. 1997). Light-dependent H^+ transport leads to activation of Viol de-epoxidase. The degree of de-epoxidation is an indication of the balance in activities of Viol

de-epoxidase and Zea epoxidase as determined by the lumen pH. Thus, the lack of a significant effect of *lsr1* on accumulation of Anth and Zea with changing irradiance (Fig. 5B) implies unaltered pH control of xanthophyll cycle-activity.

Consistent with its function in energy storage, the magnitude of the ΔpH reflects the interplay between the opposing processes of energy trapping by PSII and energy consumption by the Calvin cycle. The ΔpH thereby modulates feedback control of light capture by reaction centers, in part, through control of xanthophyll de-epoxidation. However, alternative mechanistic models for NPQ point to the importance of protonation processes distinct from operation of the xanthophyll cycle. Direct quenching by Zea and Anth is based on an apparent strict requirement for these molecules in the NPQ mechanism in vivo (Gilmore and Yamamoto 1993). Energy transfer from singlet Chl *a* to Zea is energetically possible and would be followed by thermal deactivation of the carotenoid (Demmig-Adams 1990; Frank et al. 1994). Protonation of the LHCII is postulated to facilitate binding of Zea such that the latter is in orbital contact with a bound antenna Chl *a* molecule (Gilmore et al. 1996). Horton and co-workers stress, however, that protonation in the absence of Zea can lead to nearly maximal levels of NPQ (Rees et al. 1989). Under these circumstances, acidification of the LHCII causes structural changes leading to Chl-Chl interactions that quench excitation (Crofts and Yerkes 1994). In this model quenching by Chl-Zea, H^+-Chl-Zea, and H^+-Chl-Chl are allowed and the distribution of states is regulated by allosteric interactions of xanthophylls and H^+ with the LHCII (Horton et al. 1996; Färber et al. 1997; Ruban and Horton 1999).

Either mechanistic model accomodates the conjecture that the partial loss of NPQ capacity in Lsr1$^-$ could be due to a defect in binding of Zea (and Anth) to the LHCII. This would account for the shift in the relationship between steady-state NPQ and de-epoxidation state for Lsr1$^-$ relative to WT (Fig. 6). As shown by Lokstein et al. (1994), treatment with DTT inhibits rapid-phase quenching but slow-phase quenching is unaffected. Hence, use of this inhibitor factilitates assessment of Zea-dependent NPQ in vivo. The clear effect of *lsr1* is to selectively diminish DTT-sensitive (i.e. xanthophyll-dependent) quenching (Fig. 7). Reduced affinity for Zea could be the result of diminished H^+-binding by the LHCII in the case of the first mechanistic model described above or the cause of a decrease in H^+-dependent quenching in the case of the second.

The mutant Lsr1$^-$ exhibited significantly reduced suppression of "dark" level fluorescence (i.e. higher F'_o/F_o) at the highest irradiance employed (Fig. 8). Under similar conditions DTT-insensitive quenching in the mutant constitutes a much larger proportion of total NPQ compared to WT regardless of duration of exposure to light stress (Fig. 7). In contrast to Zea-dependent quenching, DTT-insensitive phases are not associated with suppression of F'_o/F_o (Lokstein et al. 1994). This could indicate in Lsr1$^-$ a lower irradiance threshold associated with a shift from a predominantly antenna-based NPQ mechanism to one in which the PSII reaction center participates (Krause and Weis 1991). Alternatively, higher F'_o/F_o levels could result from an overburdening of the limited photoprotective capacity in the mutant leading to photodamage to the PSII reaction center (Powles and Björkman 1982).

It is unlikely that Lsr1$^-$ is associated with significant alterations in composition of the antennae systems of PSI and PSII. Mutations or illumination regimes that alter the structure of the LHCII also reduce the efficiency of excitation energy dissipation (Härtel et al. 1996). However, immunoblots provide no indication that the level of any PSII light-harvesting Chl *a*/*b* protein is affected in the mutant (Fig. 9). Likewise, Chl *b*/*a* ratios and F_v/F_{max} values are essentially identical in WT and mutant (Table 2). These observations are also inconsistent with the possibility that the apparent reduction in NPQ capacity in Lsr1$^-$ is an artifact arising from the susceptibility of measurements made with the Walz fluorometer to invariant fluorescence emission from PSI (Pfündel 1998). For any given set of conditions, a higher PSI/PSII fluorescence ratio in the mutant relative to WT could misleadingly account for lower estimates of NPQ. However, based on its computational formula, the parameter qN is not subject to this PSI-related bias (Pfündel 1998). Since values of qN were significantly lower for the mutant relative to the WT, particularly under light-stress conditions (Table 1), reduced energy-dissipation capacity in Lsr1$^-$ is clearly indicated.

We suggest that Lsr1$^-$ is a result of either impaired binding of Zea and/or H^+ by the LHCII or loss of subsequent structural changes that lead to formation of quenching states. The effect of this mutation is thus analogous to that of the NPQ inhibitor dicyclohexylcarbodiimide (Ruban et al. 1992). This inhibitor coincidentally binds to Chl-liganding glucose residues on the Lhcb4 and Lhcb5 proteins, prompting speculation that these sites are critical to ΔpH perception (Crofts and Yerkes 1994). However, in light of evidence for participation of conformational changes in the mechanism of NPQ, one must consider that alteration of gene products distinct from LHCII subunits could disrupt LHCII function by affecting protein-protein or protein-lipid interactions.

We thank Neil Hoffman (Carnegie Institute of Washington) and Judy Brusslan (California State University, Long Beach) for providing antibodies and advice on immunoblots. We also extend thanks to Francine Carland and Neil Schultes for assistance and suggestions concerning gene mapping and Southern hybridization and Carol Clark for skillful technical assistance.

References

Bell CJ, Ecker JR (1994) Simple assignment of 30 microsatellite loci to the linkage map of *Arabidopsis*. Genomics 19: 137–144

Björkman O, Niyogi KK (1998) Xanthophylls and excess-energy dissipation: A genetic dissection in *Arabidopsis*. In: G Garab (ed) Photosynthesis: mechanisms and effects, vol 3. Kluwer, Dordrecht, pp 2082–2090

Briantais J-M, Vernotte C, Picaud M, Krause GH (1980) Chlorophyll fluorescence as a probe for the determination of the

photo-induced proton gradient in isolated chloroplasts. Biochim Biophys Acta 591: 198–202

Crofts AR, Yerkes CT (1994) A molecular mechanism for qE quenching. FEBS Lett 352: 265–270

Demmig-Adams B (1990) Carotenoids and photoprotection in plants: a role for the xanthophyll zeaxanthin. Biochim Biophys Acta 1020: 1–24

Demmig-Adams B, Adams WW, Heber U, Neimanis S, Winter K, Krüger A, Czygan F-C, Bilger W, Björkman O (1990) Inhibition of zeaxanthin formation and of rapid changes in radiationless energy dissipation by dithiothreitol in spinach leaves and chloroplasts. Plant Physiol 92: 293–301

Färber A, Young AJ, Ruban AV, Horton P, Jahns P (1997) Dynamics of xanthophyll-cycle activity in different antenna subcomplexes in the photosynthetic membranes of higher plants. The relationship between zeaxanthin conversion and nonphotochemical fluorescence quenching. Plant Physiol 115: 1609–1618

Feldmann KA (1991) T-DNA insertion mutagenesis in *Arabidopsis*: mutational spectrum. Plant J 1: 71–82

Frank HA, Cua A, Chynwat V, Young A, Gosztola D, Wasielewski MR (1994) Photophysics of the carotenoids associated with the xanthophyll cycle in photosynthesis. Photosynth Res 41: 389–395

Genty B, Briantais J-M, Baker NR (1989) The relationship between the quantum yield of photosynthetic electron transport and quenching of chlorophyll fluorescence. Biochim Biophys Acta 990: 87–92

Gilmore AM, Hazlett T, Debrunner PG, Govindjee (1996) Photosystem II chlorophyll *a* fluorescence lifetimes are independent of the antenna size differences between barley wild-type and *chlorina* mutants: Comparison of xanthophyll-cycle dependent and photochemical quenching. Photosynth Res 48: 171–187

Gilmore AM, Yamamoto HY (1993) Linear models relating xanthophylls and lumen acidity to non-photochemical fluorescence quenching. Evidence that antheraxanthin explains zeaxanthin independent quenching. Photosynth Res 35: 67–78

Härtel H, Lokstein H, Grimm B, Rank B (1996) Kinetic studies on the xanthophyll cycle in barley leaves. Influence of antenna size and relations to nonphotochemical quenching. Plant Physiol 110: 471–482

Havir EA, Tausta SL, Peterson RB (1997) Purification and properties of violaxanthin de-epoxidase from spinach. Plant Science 123: 57–66

Horton P, Ruban AV, Walters RG (1996) Regulation of light harvesting in green plants. Annu Rev Plant Physiol Plant Mol Biol 47: 655–684

Krause GH, Weis E (1991) Chlorophyll fluorescence and photosynthesis: the basics. Annu Rev Plant Physiol Plant Mol Biol 42: 313–349

Lander ES, Green P, Abrahamson J, Barlow A, Daly MJ, Lincoln SE, Newburg L (1987) MAPMAKER, an interactive computer package for constructing primary genetic linkage maps of experimental and natural populations. Genomics 1: 174–181

Lichtenthaler HK (1987) Chlorophylls and carotenoids: pigments of photosynthetic membranes. Methods Enzymol 148: 350–382

Lokstein H, Härtel H, Hoffman P, Woitke P, Renger B (1994) The role of light-harvesting complex II in excess excitation energy dissipation: an in vivo fluorescence study on the origin of high-energy quenching. J Photochem Photobiol B: Biology 26: 175–184

Meinke DW, Cherry JM, Dean C, Rounsley SD, Koornneef M (1998) *Arabisopsis thaliana*: a model plant for genome analysis. Science 282: 662–682

Melis A (1999) Photosystem-II damage and repair cycle in chloroplasts: what modulates the rate of photodamage in vivo. Trends Plant Sci 4: 130–135

Meurer J, Meierhoff K, Westhoff P (1996) Isolation of high-chlorophyll-fluorescence mutants of *Arabidopsis thaliana* and their characterisation by spectroscopy, immunoblotting and Northern hybridisation. Planta 198: 385–396

Neubauer C (1993) Multiple effects of dithiothreitol on non-photochemical fluorescence quenching in intact chloroplasts. Plant Physiol 103: 575–583

Niyogi KK, Björkman O, Grossman AR (1997) *Chlamydomonas* xanthophyll cycle mutants identified by video imaging of chlorophyll fluorescence quenching. Plant Cell 9: 1369–1380

Niyogi KK, Grossman AR, Björkman O (1998) *Arabidopsis* mutants define a centrol role for the xanthophyll cycle in the regulation of photosynthetic energy conversion. Plant Cell 10: 1121–1134

Pfündel E (1998) Estimating the contribution of photosystem I to total leaf chlorophyll fluorescence. Photosynth Res 56: 185–195

Peter GF, Thornber JP (1991) Biochemical composition and organization of higher plant photosystems. II. Light-harvesting pigment proteins. J Biol Chem 266: 16745–16754

Peterson RB (1991) Analysis of changes in minimal fluorescence yield with irradiance and O_2 level in tobacco leaf tissue. Plant Physiol 97: 1388–1394

Peterson RB, Aylor DE (1995) Chlorophyll fluorescence induction in leaves of *Phaseolus vulgaris* infected with bean rust (*Uromyces appendiculatus*). Plant Physiol 108: 163–171

Powles SB, Björkman O (1982) Photoinhibition of photosynthesis: effect on chlorophyll fluorescence at 77 K in intact leaves and in chloroplast membranes of *Nerium oleander*. Planta 156: 97–107

Quick WP, Horton P (1984) Studies on the induction of chlorophyll fluorescence in barley protoplasts. II. Resolution of fluorescence quenching by redox state and the transthylakoid pH gradient. Proc R Soc London Ser B 220: 371–382

Rees D, Young A, Noctor G, Britton G, Horton P (1989) Enhancement of the ΔpH-dependent dissipation of excitation energy in spinach chloroplasts by light-activation: correlation with the synthesis of zeaxanthin. FEBS Lett 256: 85–90

Ruban AV, Walters RG, Horton P (1992) The molecular mechanism of the control of excitation energy dissipation in chloroplast membranes; inhibition of ΔpH-dependent quenching of chlorophyll fluorescence by dicyclohexylcarbodiimide. FEBS Lett 309: 175–179

Ruban AV, Horton P (1999) The xanthophyll cycle modulates the kinetics of nonphotochemical energy dissipation in isolated light-harvesting complexes, intact chloroplasts, and leaves of spinach. Plant Physiol 119: 531–542

Siefermann D, Yamamoto HY (1975) Properties of NADPH and oxygen-dependent zeaxanthin epoxidation in isolated chloroplasts. A transmembrane model for the violaxanthin cycle. Arch Biochem Biophys 171: 70–77

Sivak MN, Heber U, Walker DA (1985) Chlorophyll a fluorescence and light-scattering kinetics displayed by leaves during induction of photosynthesis. Planta 163: 419–423

van Kooten O, Snel JFH (1990) The use of chlorophyll fluorescence nomenclature in plant stress physiology. Photosynth Res 27: 121–133